Three-dimensional laser-induced photoacoustic tomography of mouse brain with the skin and skull intact

Xueding Wang, Yongjiang Pang, and Geng Ku

Optical Imaging Laboratory, Department of Biomedical Engineering, Texas A&M University, College Station, Texas 77843-3120

George Stoica

University, 3120 Texas A&M University, College Station, Texas 77843-3120

Lihong V. Wang

Department of Pathobiology, Texas A&M University, College Station, Texas 77843-5547

Received March 11, 2003

Three-dimensional laser-induced photoacoustic tomography, also referred to as optoacoustic tomography, is developed to image animal brain structures noninvasively with the skin and skull intact. This imaging modality combines the advantages of optical contrast and ultrasonic resolution. The distribution of optical absorption in a mouse brain is imaged successfully. The intrinsic optical contrast reveals not only blood vessels but also other detailed brain structures, such as the cerebellum, hippocampus, and ventriculi lateralis. The spatial resolution is primarily diffraction limited by the received photoacoustic waves. Imaged structures of the brain at different depths match the corresponding histological pictures well. © 2003 Optical Society of America

OCIS codes: 170.5120, 170.3880, 170.0110, 110.6880, 170.3010.

Optical contrast is sensitive not only to different soft tissues that have different optical properties but also to functional changes, such as blood hemoglobin concentration and tissue oxygenation, in biological tissues. Because optical contrast has several potential advantages over existing methods of neuroimaging,[1,2] optical imaging has been employed in clinical applications in neuroscience, including investigations of neuroanatomy[3] and neuroactivity.[1,4,5] However, because of the overwhelming scattering of light in biological tissues, past approaches to imaging brain architectures noninvasively with optical contrast were severely restricted by the unsatisfactory spatial resolution. Another method of pure optical imaging, which is based on invasive open-skull photography, can map brain surfaces precisely but cannot provide depth resolution.[6,7]

Photoacoustic tomography (PAT), a technique for imaging optical properties in biological tissues noninvasively, combines the merits of both light and ultrasound.[8–11] We report in this Letter three-dimensional (3-D) imaging of mouse brain structures as well as vascular distributions achieved noninvasively through a high-resolution laser-induced PAT system. PAT images the brain architecture based on high intrinsic optical contrast while utilizing the diffraction-limited high spatial resolution of ultrasound. Reconstructed maps of optical absorption in the horizontal cross sections (planes) of the brain at different imaging depths matched the corresponding histological pictures well, demonstrating that PAT is a promising imaging modality for the study of the functional and structural organization of the brain.

When light energy is absorbed by a biological tissue sample, a small temperature rise in the tissue causes thermoelastic expansion that leads to ultrasonic waves. The initial ultrasonic pressure is linearly proportional to the local optical absorption (also called optical energy deposition) in the tissue. To produce photoacoustic (PA) waves efficiently, the laser pulse must be short. The setup for noninvasive transdermal and transcranial 3-D PAT of a mouse brain is shown in Fig. 1. A Nd:YAG laser (Brilliant B, Bigsky) operating at a wavelength of 532 nm with a FWHM of 6.5 ns and a pulse repetition rate of 10 Hz was employed as the energy source. The laser beam was expanded and homogenized by a piece of concave lens and a piece of ground glass before it fully illuminated the mouse head. The incident energy density of the laser beam was controlled to <10 mJ/cm^2, which induced a temperature rise in the skin that was estimated to be <20 mK.

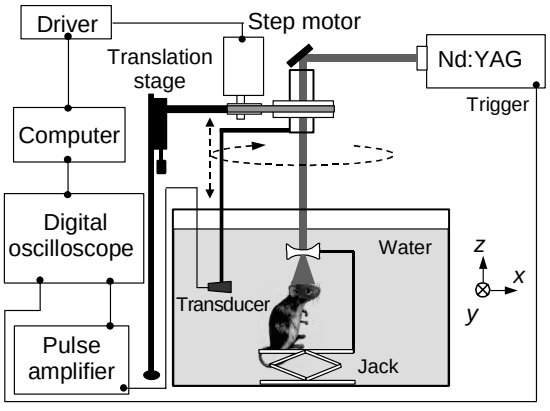

Fig. 1. Setup for noninvasive transdermal and transcranial 3-D PAT of a mouse brain.

0146-9592/03/191739-03$15.00/0

A nonfocused ultrasonic transducer (XMS-310, Panametrics) with a central frequency of 10.4 MHz, a bandwidth of 100% at −6 dB (5.2–15.6 MHz), and an active element of 2 mm in diameter was used to detect the PA signals. The transducer, driven by a computer-controlled step motor, scanned around the mouse head in horizontal planes with a radius of 2.8 cm and a step size of 2°. The transducer and the step motor were fixed on a translation stage for scanning along the z axis, where the scanned range was 4.1 cm with a step size of 0.635 mm. The circular scan in the x–y plane in combination with the linear scan along the z axis constituted a cylindrical scan around the mouse head. The transducer and the mouse were immersed in water for the coupling of PA signals. If *in vivo* experiments are conducted, the mouse can breathe through an aerophore. The PA signals detected by the transducer were received by a low-noise pulse preamplifier (500 PR, Panametrics) and then sent to an oscilloscope (TDS-640A, Tektronix). Finally, a computer collected the digitized PA signals to reconstruct the distribution of optical absorption within the mouse brain. The brains of adult BALB/c mice (Charles River Breeding Laboratories, ~50 g) were imaged *in situ* by PAT. Before the experiment, the hair on the heads of the mice was removed gently with hair remover lotion.

Our recent development of an accurate reconstruction algorithm[12] and the configuration of laser illumination relative to the planes of circular scans in combination with the full-view detection of each circular scan played a crucial role in achieving the high-quality images reported here. When the distance between the transducer and the sample is much larger than the wavelengths of the PA waves that are useful for imaging (as was true in our experiments), we use the following 3-D reconstruction formula:

$$A(\mathbf{r}) = -\frac{\beta}{2c^4\pi C_P}\iint_{S_0} \mathrm{d}S_0\,\frac{1}{t}\,\frac{\partial p(\mathbf{r}_0,t)}{\partial t}\bigg|_{t=|\mathbf{r}_0-\mathbf{r}|/c}, \quad (1)$$

where $A(\mathbf{r})$ denotes the optical absorption within the sample at position $\mathbf{r}$, β is the thermal coefficient of volume expansion, c is the acoustic speed, C_P is the specific heat, $p(\mathbf{r}_0,t)$ is the acoustic pressure at position $\mathbf{r}_0$ and time t, and S_0 is the cylindrical surface of the scanned cylinder.

3-D PAT imaging of a mouse brain was achieved noninvasively with the skin and skull intact, as shown in Fig. 2. The thickness of the skin and skull covering the brain is ~0.5 mm.

Figure 2A shows the imaged cross section corresponding to the cortical surface of the mouse brain, where the vascular distribution in the superficial cortex can be seen clearly with high optical contrast. The smallest vessels in the superficial cortex that can be seen with this PAT system have a diameter of ~30 μm, which presents a width of ~90 μm in the image. This result shows that the spatial resolution of the PAT system is ~60 μm. Because the upper-limit frequency of the −6-dB band of the ultrasound transducer is 15.6 MHz, the theoretical diffraction-limited resolution is ~58 μm.[13] Therefore, the spatial resolution of this PAT system in mouse brain imaging has approached its theoretical limit. This also demonstrates that the resolution of PAT is limited by the bandwidth of detected PA signals rather than by optical diffusion as is the case in pure optical imaging.

The images in Figs. 2B–2F present the interior brain structures underneath the superficial cortex.

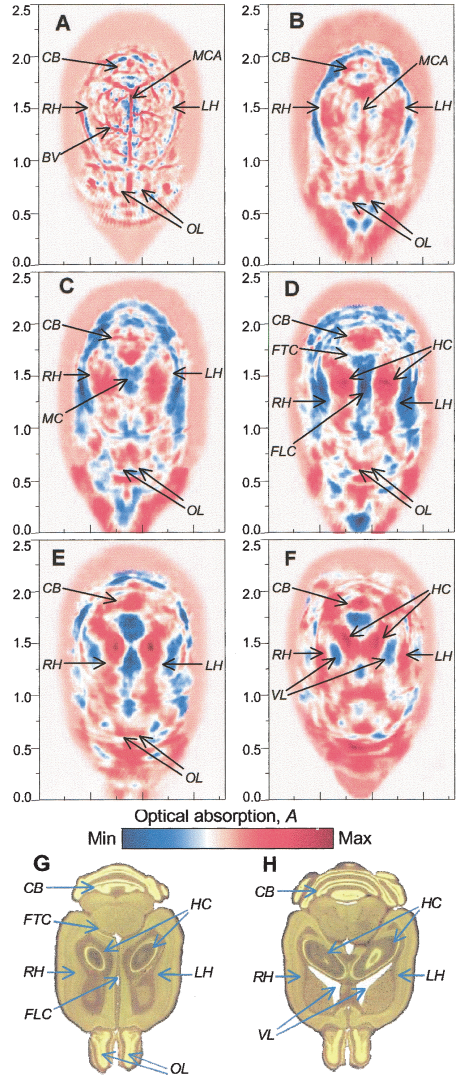

Fig. 2. Noninvasive 3-D PAT of a mouse brain achieved with the skin and skull intact. The images show horizontal cross sections from the dorsal to the ventral part of the brain, where the imaging depth is A, 0.5 mm; B, 2.0 mm; C, 3.5 mm; D, 5.0 mm; E, 6.5 mm; and F, 8.0 mm from the top surface of the mouse's head, with a constant interval of 1.5 mm. The size of each image is 1.8 cm × 2.5 cm. A color bar shows the magnitude of optical absorption, where the red areas (such as blood vessels) indicate tissues with comparatively higher optical absorption. Histological pictures in G and H are presented for comparison with the corresponding images in D and F. In the PAT images and histological pictures, the major characteristic tissue structures in the mouse brain are indicated. BV, blood vessel; CB, cerebellum; FLC, fissura longitudinalis cerebri; FTC, fissura transversa cerebri; HC, hippocampus; LH, left hemisphere; MC, mesencephalon; MCA, middle cerebral artery; OL, olfactory lobes; RH, right hemisphere; VL, ventriculi lateralis.

For illustration, the images in Figs. 2D and 2F are compared with their corresponding histological pictures in Figs. 2G and 2H.[14] A satisfactory match between them can be seen, which demonstrates that the characteristic tissue structures in the mouse brain can be imaged clearly and accurately through the skin and skull with our PAT system. The absorption coefficient of whole blood (>100 cm^{-1} at the 532-nm wavelength) is much larger than the averaged absorption coefficient of the gray and white matter of the brain (~ 0.56 cm^{-1} at 532-nm wavelength).[15,16] Therefore, the contrast of the PAT images presented here actually reveals the blood hemoglobin concentrations in various brain tissues.

In this Letter we have demonstrated that our 3-D PAT provides a noninvasive method for localizing and quantifying regional optical properties of brain tissues through the skin and skull with high ultrasonic resolution. The completely noninvasive advantage of PAT improves data consistency while providing savings in labor and animal resources. Since the 3-D PAT system described here was realized through cylindrical scanning of a single-element transducer, the time resolution was not high. The period for each circular scan was 15 min, and the total time for 3-D PA signal detection was $\sim$16 h. In the future, PAT based on an ultrasonic transducer array, instead of a single-element transducer, will permit real-time imaging. Further imaging of the superficial cortex of human brains, albeit significantly more difficult, is also possible with near-infrared lasers. PAT, as a novel functional imaging modality in addition to functional magnetic resonance imaging and positron emission tomography, can potentially advance neuroscience significantly.[17] Since the brain is highly responsive to changes in the blood oxygenation level, the application of PAT will be greatly broadened when multiple wavelengths are employed to realize oxygen-dependent imaging with high temporal and high spatial resolution.

This study was sponsored in part by the U.S. Department of Defense, the National Institutes of Health, the National Science Foundation, and the Texas Advanced Research Program. L. V. Wang's e-mail address is LWang@tamu.edu.

References

1. A. Villringer and B. Chance, Trends Neurosci. **20,** 435 (1997).
2. G. Gratton, M. Fabiani, P. M. Corballis, D. C. Hood, M. R. Goodman Wood, J. Hirsch, K. Kim, D. Friedman, and E. Gratton, Neuroimage **6,** 168 (1997).
3. A. Grinvald, E. Lieke, R. D. Frostig, C. D. Gilbert, and T. N. Wiesel, Nature **324,** 361 (1986).
4. B. Chance, Z. Zhuang, C. UnAh, C. Alter, and L. Lipton, Proc. Natl. Acad. Sci. USA **90,** 3770 (1993).
5. A. Villringer, J. Planck, C. Hoch, L. Schleinkofer, and U. Dirnagl, Neurosci. Lett. **154,** 101 (1993).
6. R. D. Frostig, E. E. Lieke, D. Y. Ts'o, and A. Grinvald, Proc. Natl. Acad. Sci. USA **87,** 6082 (1990).
7. M. M. Haglund, G. A. Ojemann, and D. W. Hochman, Nature **358,** 668 (1992).
8. C. G. A. Hoelen, F. F. M. de Mul, R. Pongers, and A. Dekker, Opt. Lett. **23,** 648 (1998).
9. R. A. Kruger, D. R. Reinecke, and G. A. Kruger, Med. Phys. **26,** 1832 (1999).
10. R. O. Esenaliev, A. A. Karabutov, and A. A. Oraevsky, IEEE J. Sel. Top. Quantum Electron. **5,** 981 (1999).
11. K. P. Köstli, D. Frauchiger, J. J. Niederhauser, G. Paltauf, H. P. Weber, and M. Frenz, IEEE J. Sel. Top. Quantum Electron. **7,** 918 (2001).
12. M. Xu, Y. Xu, and L. V. Wang, "Time-domain reconstruction algorithms and numerical simulations for thermoacoustic tomography in various geometries," IEEE Trans. Biomed. Eng. (to be published).
13. M. Xu and L. V. Wang, Phys. Rev. E **67,** 056605 (2003).
14. G. D. Rosen, A. G. Williams, J. A. Capra, M. T. Connolly, B. Cruz, L. Lu, D. C. Airey, K. Kulkarni, and R. W. Williams (2000), The Mouse Brain Library @ www.mbl.org.
15. J. K. Barton, G. Frangineas, H. Pummer, and J. F. Black, Photochem. Photobiol. **73,** 642 (2001).
16. P. VanderZee, M. Essenpreis, and D. T. Delpy, Proc. SPIE **1888,** 454 (1993).
17. X. Wang, Y. Pang, G. Ku, X. Xie, G. Stoica, and L. V. Wang, Nature Biotechnol. **21,** 803 (2003).